Cell and Tissue Research (2019) 378:255 265
https://doi.org/10.1007/s00441-019-03054-2

REGULAR ARTICLE

# Experimental pulmonary fibrosis was suppressed by microRNA-506 through NF-kappa-mediated apoptosis and inflammation

Min Zhu[1] · Yunxia An[1] · Xiaoju Zhang[1] · Zheng Wang[1] · Hongyan Duan[2]

Received: 29 October 2018 / Accepted: 28 May 2019 / Published online: 18 June 2019


## Abstract

Fibrosis in the lungs usually occurs in the initial phase of acute respiratory distress syndrome (ARDS), which exacerbates poor prognosis among patients. MicroRNAs (miRs) have the ability to modulate the expression profiles of many genes, thus essentially altering cell phenotypes. We hypothesize that miRs may be involved in the development of lung fibrosis in mice. In this study, mice were treated with lipopolysaccharide (LPS) to establish the lung fibrosis animal model. Hematoxylin and eosin (H&E) staining and western blot (WB) were performed to confirm the successful establishment of the model. Quantitative PCR (qPCR) and WB were utilized to monitor the expression of miRs and proteins. A dual-luciferase reporter assay was used to detect the interaction between miR and genes. We observed miR-506 downregulation in lung tissues during lung fibrosis after ARDS rat modeling by LPS exposure. We also observed that its expression level was similar to that observed in TGF-β1-induced human MRC-5 cells. The proportion of apoptotic cells decreased, while levels of inflammatory cytokines were upregulated in lung tissues during lung fibrosis and in fibroblasts after TGF-β1 treatment. In order to elucidate the possible role of miR-506, it was overexpressed in mice with ARDS. It was revealed that miR-506 significantly ameliorated the degree and spread of pulmonary damage stimulated by LPS. miR-506 also induced apoptosis in vivo and in vitro, while also ameliorating the inflammatory response. Notably, p65, a subunit of NF-κB, acts as a target of miR-506. p65 expression was downregulated in TGF-β1-treated MRC-5 cells upon transfection with miR-506 mimic. Indeed, the 3′-UTR of human p65 contained functional human miR-506-responsive sequences. LPS induction and TGF-β1 stimulation in mice led to p65 upregulation. In addition, p65 knockdown in the ARDS mouse model partially ameliorated the severity of lung lesions, induced apoptosis and reduced inflammation in lung tissue. Our findings revealed that miR-506 could be an important modulator of apoptosis and inflammation and a regulator of lung fibrosis.

**Keywords** Pulmonary fibrosis · LPS · miR-506 · p65 · Apoptosis

✉ Hongyan Duan
hongyanduanyx@163.com

Min Zhu
golday57@163.com

Yunxia An
Simone0398@126.com

Xiaoju Zhang
15038207533@163.com

Zheng Wang
21903582@qq.com

[1] Department of Respiratory and Critical Care Medicine, Henan Provincial People's Hospital, People's Hospital of Zhengzhou University, Zhengzhou, Henan, China

[2] Department of General Medicine, Henan Provincial People's Hospital, People's Hospital of Zhengzhou University, NO.7 Wei Wu Road, Jinshui District, Zhengzhou 450003, Henan, China

## Introduction

Acute respiratory distress syndrome (ARDS) is an emerging respiratory dysfunction involving persistent hypoxemic reactions (Ragaller and Richter 2010). Previous studies have reported that in the initial phase of ARDS (within the first 7 days), pathological alterations in the lungs primarily include exudation events. The appearance of collagenous fibers is increased after 7 days, with the eventual development of fibrosis in the lungs (Cunningham 1991). Nevertheless, recent studies have also indicated that lung fibrosis could occur in the initial phase of ARDS (Marshall et al. 2000). Early development of fibrosis in lung tissues is associated with poor prognosis among ARDS patients (Burnham et al. 2014). Hence, it is important to find therapeutic alternatives and more effective

ARDS prognosis tools via the investigation of early lung fibrosis.

Several interconnected signaling pathways in the mucous membrane are relevant to early fibrous activity (Rockey et al. 2015). The activated TGF-β is key in the fibrogenic reaction (Munger et al. 1999). Its pleiotropism notwithstanding, TGF-β has been shown to trigger the relevant signal in neighboring lung epithelial cells (Degryse et al. 2011; Li et al. 2011) and overexpressed TGF-β has been shown to be associated with pulmonary fibrosis (Lee et al. 2004; Sime et al. 1997). Activation of the TGF-β signaling pathway leads to the transcription of pro-fibrosis regulators (Leask and Abraham 2004). Nevertheless, TGF-β leads to the death of epithelial cells, partially promoting the fibrous proliferative reaction (Lee et al. 2004). Other events such as extreme endoplasmic reticulum stress, cellular apoptosis and other symptoms related to age, such as shortening of telomere length and aging of cells, also lead to fibrosis formation (Lawson et al. 2011; Leask and Abraham 2004). Owing to the intricacy of signals that cause fibrosis, therapeutic strategies are highly likely to interfere with a number of signaling channels. Nintedanib targets several tyrosine kinases and has been shown to be capable of mitigating idiopathic pulmonary fibrosis (IPF) development (Richeldi et al. 2014). However, current therapeutic strategies are insufficient to achieve a complete cease of fibrosis development.

miRNAs (miRs) are short non-coding RNAs with a simple structure consisting of a single strand, 18 to 22 nucleotides long and are widely found in nature (Ambros 2004; Carrington and Ambros 2003). Many investigations have highlighted the critical role of miRs in multiple biological reactions, such as cell death and migration of cancer cells. miR-506 is downregulated in several types of cancers and serves as a tumor inhibitor by targeting key oncogenes, such as N-Ras, SPHK1, ETS-1 and ROCK1. It therefore mediates significant cancer-related events, such as cell generation, apoptosis, aging, invasion, metastasis and drug resistance (Li et al. 2016). miR-506 overexpression inhibits cell proliferation and promotes osteosarcoma cell apoptosis by targeting astrocyte elevated gene-1 (Yao et al. 2016).

Previous studies have also indicated that miRs play an important role in epithelial-mesenchymal transition (EMT), a critical step in the fibrogenic process (Chapman 2011), by negative regulation of its target (Ding 2014). A number of studies have validated the role of miR-506 as a primary EMT suppressor by directly targeting SNAI2, the E-cad transcriptional suppressor. miR-506 has the ability to inhibit EMT and metastasis, therefore indicating a potential novel therapeutic strategy (Sun et al. 2014). Researchers have found that overexpressed miR-506 could suppress TGF-β-stimulated EMT and inhibit adherence, aggression and relocation of MDA-MB-231 cells (breast cancer cell line) (Arora et al. 2013). In stomach cancer, miR-506 overexpression suppressed the EMT of cancerous cells and was implicated in the inhibition of the ETS1 target involved in metastasis and vasculogenesis (Li et al. 2015).

In our study, we established an experimental animal model of early-stage lung fibrosis using lipopolysaccharide (LPS). This was done to evaluate the expression levels of various genes involved in miR-506/NF-κB (p65) signaling pathways and to study the influence of miR-506/p65 on early-stage lung fibrosis via apoptotic and inflammatory responses.

## Materials and methodology

### Animals

C57BL/6 mice 20–25 g in weight were acquired from the Vital River, Beijing, China. LPS from Sigma-Aldrich (*Escherichia coli* 055: B5) (St. Louis, USA) was used. TGF-β was procured from Pepro Tech (Rocky Hill, USA). Each procedure was approved by the Animal Care and Use Committee of the People's Hospital of Zhengzhou University and was in conformity with the guidelines of the National Institute of Health (No 81004).

### Experimental model

The experiment on early lung fibrosis was conducted in animal models by LPS induction using the revised approach, as mentioned above (Li et al. 2009). Briefly, eight mice from every test group were anesthetized by intraperitoneally injecting 0.8% pentobarbital at 200 μL per 10 g of the animal's weight. Orotracheal intubation was then performed with a puncture needle. LPS was administered to the lung through an intratracheal tube at a dosage of 1.5 mg/kg. This was dispersed evenly inside the lung by the mice. The tube was then removed. LPS was intraperitoneally injected at a dosage of 3 mg/kg after 24 h, followed by injection through the intratracheal tube after 48 h. Normal saline was used in equal amounts for the control group. After 21 days of LPS treatment, the mice were sacrificed. Alveolar lavage was performed prior to the harvest of lung tissues. The tissues from the left lung were utilized for a cytohistological assay and those from the right were used for mRNA/protein assessment.

### Recombinant lentiviral miR-506 or p65 shRNA vector transduction

Both lentivirus overexpressing miR-506 and the lentiviral vector carrying p65 shRNA were purchased from

Genomeditech (Shanghai, China). Three shRNA sequences targeting the mouse p65 coding area were developed and lentivirus carriers were developed accordingly. The negative control (NC) was built using one ineffective RNA sequence. Lentivirus-miR-506-mimic, lentivirus-shRNA-p65, lentivirus-NC-mimic and lentivirus-NC were injected endotracheally into the lungs of C57BL/6 mice, using eight mice from every group. Post-gene transduction mice were injected with LPS, as mentioned above. After being treated with LPS for 21 days, mice were sacrificed to harvest the pulmonary tissues.

## Hematoxylin and eosin (H&E) staining

After inflation with neutral-buffered formalin, the left lower lungs of the mice were kept for over 48 h and then embedded in paraffin. They were cut into 5-μm-thick sections, which were processed by H&E staining to evaluate the spread and intensity of the lesions. To evaluate the fundamental changes in the lungs induced by the different treatments, the thickness of the pulmonary alveolar wall, cellular proliferation, inflammatory injury, collagen sediment and the degree of lung fibrosis were observed under a microscope.

## Hydroxyproline assay

Collagen synthesis was determined by a hydroxyproline assay (Yang et al. 2010). Lung samples were homogenized in 2 mL phosphate-buffered saline (PBS). A 1-mL aliquot was hydrolyzed with 6 N HCl at 110 °C for 18 h, following the Woessner method (Woessner Jr 1961). Following this, 25-μL aliquots were added to 1 mL of 1.4% chloramine T (Sigma-Aldrich, St. Louis, MO, USA), 10% 2-propanol and 0.5 M sodium acetate of pH 6.0. After 20 min of incubation at room temperature, 1 mL Erlich's solution (1 M *p*-dimethyl-amino-benzaldehyde in 70% 2n-propanol and in 20% perchloric acid) was added, followed by a 15-min incubation at 65 °C. Samples were read in a spectrophotometer (ELx800 Absorbance Microplate Reader, BioTek Instrument, Luzen, Switzerland). The amount of hydroxyproline was determined against a standard curve. Data are expressed in micrograms per gram of lung tissue.

## Quantitation of IL-6 by ELISA

IL-6 serum levels were determined using ELISA kits (BioSource International, Camarillo, CA, USA) according to the manufacturer's instructions. Lung samples were drawn from healthy control mice and from mice that underwent different treatments. The lung samples were placed on ice for 15 min and allowed to gently homogenize, before centrifugation at 5000*g* for 10 min. Samples were then used in various dilutions for ELISA.

## Cell lines and treatment

Human bronchial epithelial (HBE) and MRC-5 pulmonary fibroblast cells were purchased from the American Type Culture Collection (Manassas, USA). The cells were cultivated in Dulbecco's modified Eagle medium, supplemented with 10% (*v*/*v*) fetal bovine serum (Gibco, Grand Island, NY) and 0.1% penicillin plus streptomycin, in a 5% $CO_2$-humidified container at 37 °C. The MRC-5 fibroblasts were cultured with TGF-β1 (1 ng/mL; Sigma-Aldrich) for 2 days. Meanwhile, total RNA/protein levels were evaluated following the manufacturer's instructions.

## Transfection

MiR-506 mimic (Mimic), miR-506 negative control (NC-mimic), miRNA-506 inhibitor (Inhibitor) and its negative control (NC-inhibitor) were purchased from RiboBio (Guangzhou, China). Cells were seeded and cultured for 24 h before undergoing transfection with the abovementioned RNA oligonucleotides using Invitrogen's Lipofectamine-2000, following the manufacturer's guidelines. Around 24–48 h post transfection, the cells were ready for further experimentation.

## Western blotting (WB)

RIPA buffer (pH 8.0) containing 0.1% sodium dodecyl sulfate (SDS), 150 mM NaCl, 1% NP-40 and 50 mM Tris-HCl was used for the preparation of whole cell lysate. A bicinchoninic acid protein quantitation kit was used for protein quantification, followed by the separation of proteins by sodium dodecyl sulfate-polyacrylamide gel electrophoresis (SDS-PAGE) using a 10% polyacrylamide gel. Proteins were then transferred to PVDF membranes (Millipore, MA, USA). Immunoblots were prepared using 5% bovine serum albumin at 25 °C for 1 h. They were incubated with primary antibodies at 4 °C for 24 h. Following incubation, the blots were treated with corresponding secondary antibodies at 25 °C for 1 h. Immunoreactivity was measured by the Super Signal West Femto Maximum Sensitivity Substrate Kit (Thermo Scientific, MA, USA). Images were taken using the C-DiGit Blot Scanner.

## Quantitative real-time PCR (qPCR)

Total RNAs (100 ng) of the tissues were isolated using Invitrogen's Trizol solution, following the manufacturer's instructions. RNA was quantified using Nanodrop-2000 at OD260. Reverse transcription and mRNA qPCR were carried out with MMLV 1st Strand Kit, Oligo (dT) 20 primer and SYBR Select Master Mix

(Invitrogen). The qPCR of miR was carried out using the TaqMan MicroRNA Reverse Transcription Kit and TaqMan miR assessment for miR-506 and U6 and TaqMan Universal Master Mix II without UNG. PCR was carried out with the Stratagene MX3005P instrument. Cycle parameters were 95 °C for 10 min, 40 cycles at the same temperature for 15 s. Annealing and stretching were then performed at 60 °C for 40 s. The gene expression $2^{-}$levels of mRNA/miR-506 in every group were normalized with the internal control of GAPDH/U6. Fold alteration was measured by the equation $2^{-\Delta\Delta CT}$. All experiments were conducted in triplicate to ensure accuracy.

### TUNEL staining

TUNEL staining was performed in formalin-fixed, paraffin-embedded lung sections using an In Situ Cell Death Detection kit, POD (Roche Diagnostics), according to the manufacturer's protocol. Positively stained apoptotic cells were counted randomly in five microscopic fields from at least three slides of each mouse under a light microscope. The percentage of TUNEL staining represented the number of TUNEL-positive cells in a field, with a total of 100 nuclei.

### Apoptosis assay

Cell apoptosis was measured using the BD Pharmingen™ Annexin V-FITC & PI apoptosis assay kit. After transfection, cells were resuspended in 20 μL of binding buffer and then incubated for 20 min with 5 μL of PI and 10 μL of Annexin V-FITC in dark conditions. Cell death was evaluated using flow cytometry (FC).

### Dual-luciferase reporter assessment (DLRA)

3′-UTR luciferase reporter assessment was carried out to verify miR-506's target gene using the wild-type (WT) and mutant (MU) 3′-UTR of p65. The sequences of Renilla and firefly luciferases were built for reporter and calibration fluorescence (Rluc & Luc), respectively. Cells were transfected with miRNA mimic/NC and fluorescence carriers and cultivated for 36 h. Luciferase activity was evaluated via the dual-luciferase reporter assessment.

### Statistical assessment

Data are presented as the mean ± standard deviation (SD). The statistical significance among the groups was measured via Student's *t* tests. Disparity between groups was determined by one-way variance assessment coupled with Dunnett's test. Various groups were compared through one-way variance assessment coupled with Bonferroni's test. Statistical assessment was carried out using GraphPad Prism (ver. 7; San Diego, USA). A *P* value of 0.05 was considered to indicate statistically significant differences between groups.

## Result

### In vivo modeling

H&E staining demonstrated normal pathological morphology in the pulmonary tissues of the control group. In the LPS-treated group, the alveolar walls were gently extended and at 21 days post LPS injection, pro-inflammatory cells had permeated the alveolar space. The alveolar septum was eliminated upon subsiding of the inflammation, leading to destruction of the alveolar organ on the 21st day (Fig. 1a). A previous study showed that LPS treatment modulated the expression of proteins associated with epithelial-mesenchymal transition, which is involved in the development of early lung fibrosis (Cao et al. 2018a). Our data showed that in the LPS-treated group, protein levels of the epithelial cell marker (E-cadherin) decreased, while that of mesenchymal cell markers increased (α-SMA & Vimentin) (Fig. 1b, c). Our findings were also supported by the qPCR results, suggesting that LPS treatment facilitated the EMT process (Fig. 1d). In addition, we found that miR-506 levels were significantly downregulated in pulmonary tissues during the development of LPS-triggered early lung fibrosis (Fig. 1e). Previous studies have reported that TGF-β1 is one of the many elements that participate in pulmonary fibrosis generation (Kang et al. 2007; Zhang et al. 1996). Therefore, MRC-5 and HBE cells producing recombinant TGF-β1 protein were generated. The figures reveal that TGF-β1 decreased miR-506 production in MRC-5 cells but not in HBE cells (Fig. 1f).

### Overexpression of miR-506 partially ameliorated lung fibrosis

To understand the possible impact of miR-506 on the progression of LPS-triggered lung fibrosis, mouse samples were prepared. To upregulate miR-506 levels in vivo, lentivirus-miR-506-mimic or lentivirus-NC-mimic was injected intratracheally on the first day. They were injected through the vein on the 7th, 14th and 21st day post LPS induction and the lungs of the mice were excised at day 28. Unsurprisingly, 28 days post LPS induction, miR-506 levels had decreased. Nevertheless, the addition of lentivirus-miR-506 led to elevated miR-506 levels in comparison with those of the LPS + NC group (Fig. 2a).

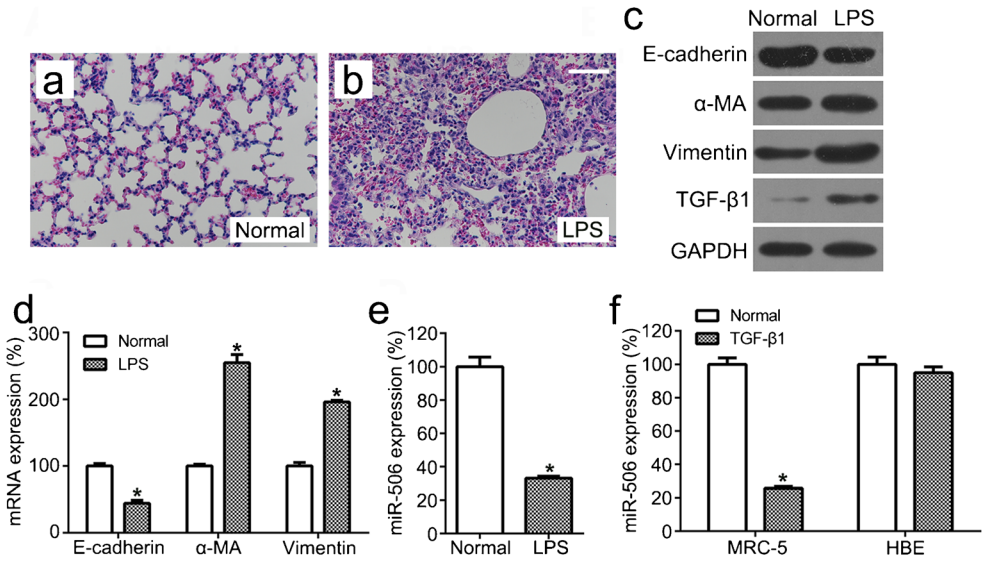


**Fig. 1** Pathological alterations in pulmonary tissue and miR-506 levels in lung tissue and cells at early stages of lung fibrosis. H&E (**a**, **b**) staining of pulmonary tissue in a mouse sample with early lung fibrosis. Western blot (WB) (**c**) analysis was used to explore the expression levels of EMT-related proteins (E-cadherin, α-MA and vimentin). qPCR was conducted to measure the mRNA levels of E-cadherin, α-MA, vimentin (**d**) and miR-506 (**e**). The fibroblasts MRC-5 and HBE were processed with TGF-β1 in 1 ng/mL (Sigma-Aldrich) for 48 h (**f**). Total RNA/protein was extracted. qPCR was conducted to determine the expression levels of miR-506. Data are recorded as mean ± SD. $*P < 0.05$, in comparison with the indicated group. Scale bar, 20 μM

Histological analyses also revealed significant pathological changes on the 21st day after miR-506 overexpression. H&E staining showed prominent structural changes, with a progressive increase in parenchymal distortion and

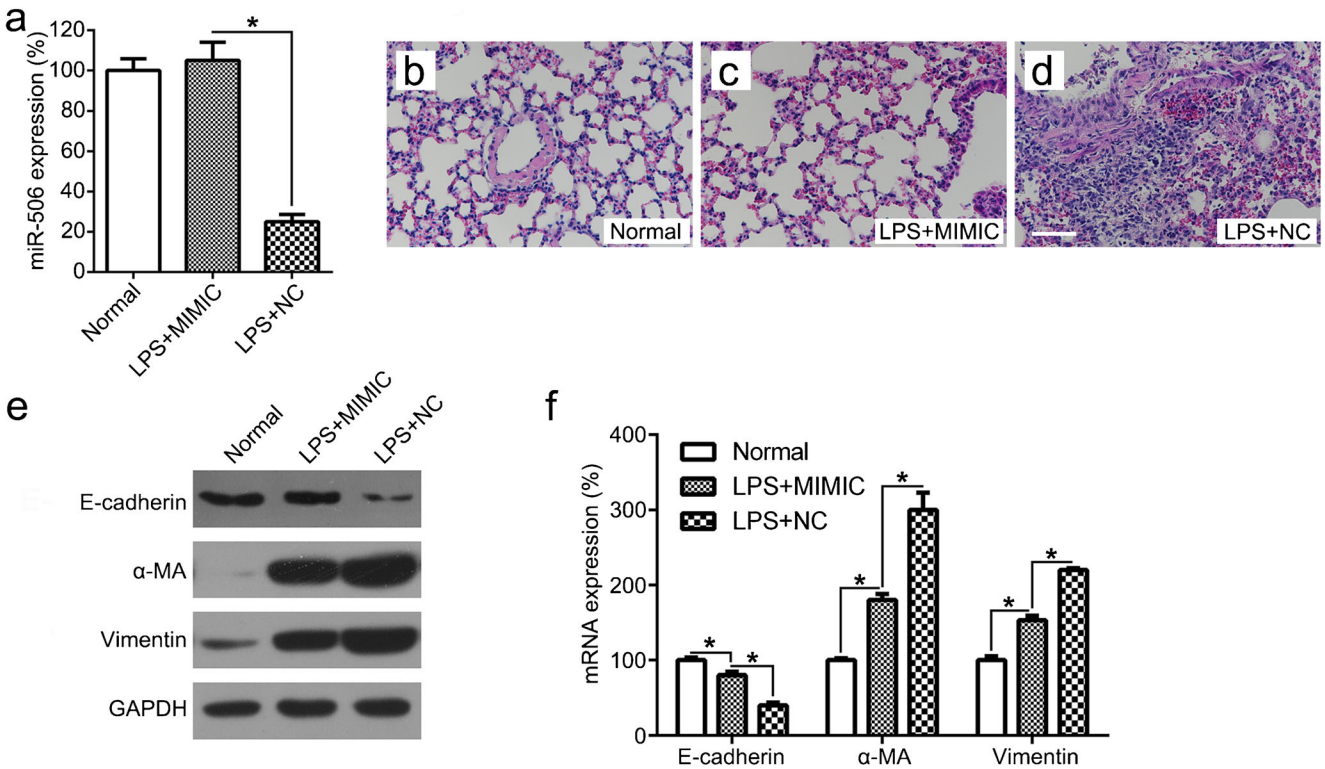


**Fig. 2** miR-506 overexpression ameliorated the pathology in lung tissue of mice with lung fibrosis. Lentivirus-miR-506 and lentivirus-NC were injected into the lungs of C57BL/6 mice pretreated with LPS (**a**). qPCR was used to confirm the overexpression of miR-506. H&E staining (**b**, **c**, **d**) in lung tissue of mice with early lung fibrosis administered with lentivirus-miR-506 and lentivirus-NC. WB (**e**) and qPCR (**f**) analyses were carried out to examine the protein and mRNA levels of EMT-related proteins (E-cadherin, α-MA and Vimentin). Data are recorded as the mean ± SD. $*P < 0.05$, in comparison to the indicated group. Scale bar, 20 μM

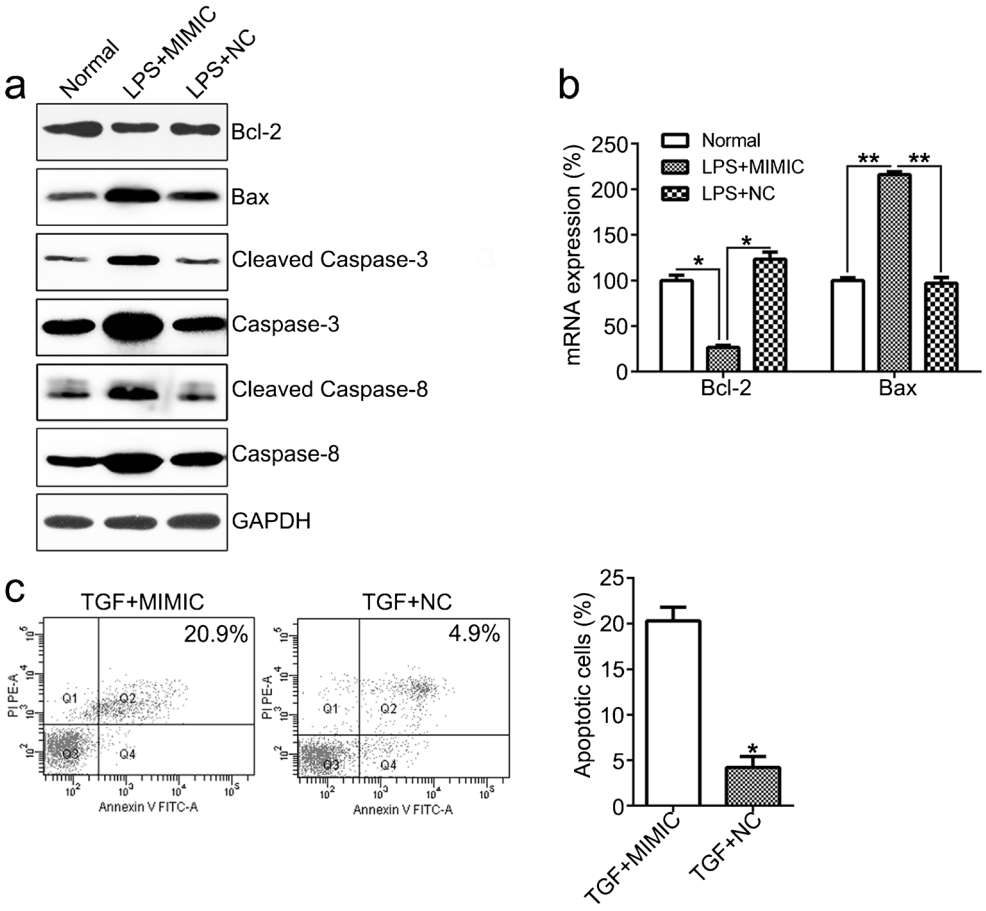


**Fig. 3** miR-506 overexpression enhanced apoptosis in lung tissue of mice with lung fibrosis and TGF-β1-treated MRC-5 cells. Intratracheal injection of lentivirus-miR-506 and lentivirus-NC was administered to the pulmonary tissues of C57BL/6 mice pretreated with LPS. WB (**a**) was used to evaluate the expression levels of Bax, Bcl-2, caspase-3, caspase-8 and their cleaved forms. qPCR (**b**) was done to assess the mRNA levels of Bcl-2 and Bax. The MRC-5 fibroblasts (**c**) were treated with TGF-β1 (1 ng/mL) for 48 h and then transfected with miR-506-mimic and NC-mimic. Annexin V-FITC & PI FC were carried out to detect the proportion of apoptotic cells. Apoptotic cells are shown in the upper right of each plot. An analysis of the apoptotic rate of cells in all groups is shown in the right panels. Data are presented as the mean ± SD. $^{*}P < 0.05$, $^{**}P < 0.01$, in comparison to the indicated group

fibrotic foci at day 21. Meanwhile, miR-506 overexpression significantly ameliorated the pathology of LPS-induced lung fibrosis (Fig. 2b, c, d). Notably, miR-506 has been reported to possess the ability to inhibit EMT and cancer cell migration (Sun et al. 2014). Nevertheless, the mechanism by which miR-506 affects lung fibrosis is still unclear. WB and qPCR analyses demonstrated that ectopic expression of miR-506 led to upregulated E-cadherin and downregulated α-SMA and vimentin at the protein and mRNA levels, in comparison with the NC group (Fig. 2e, f). This demonstrates the regulatory role of miR-506 in LPS-induced lung fibrosis in vivo.

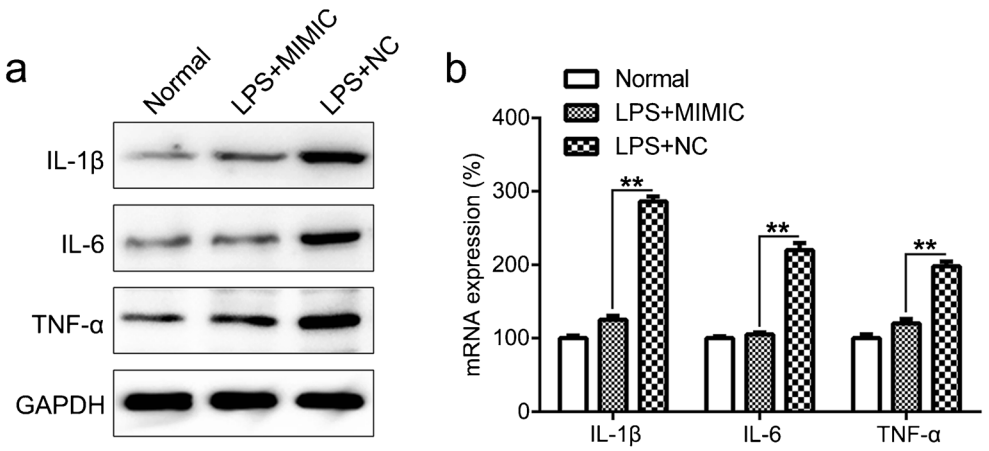


**Fig. 4** miR-506 overexpression decreased pro-inflammatory factors in the lung tissue of mice with pulmonary fibrosis. Lentivirus-miR-506 and lentivirus-NC were injected intratracheally into the pulmonary tissue of C57BL/6 mice pretreated with LPS. WB (**a**) and qPCR analyses (**b**) were performed to examine the expressions of IL-6, IL-1β and TNF-α at the protein and mRNA levels, respectively. Data are presented as the mean ± SD. $^{**}P < 0.01$, in comparison to the indicated group

## miR-506 overexpression induced apoptosis during pulmonary fibrosis in vivo and in vitro

We examined the mechanism of action of miR-506 during pulmonary fibrosis. We first confirmed that the transfection of lentivirus-506-mimic led to an increase in miR-506 levels in LPS-treated mice (Fig. 2a). We then determined the influence of miR-506 on Bax and Bcl-2 expression levels, as well as on caspase-3 and caspase-8 activity. miR-506 overexpression led to downregulated anti-apoptotic Bcl-2 expression and upregulated pro-apoptotic Bax expression, as compared with those in the normal and NC groups. Additionally, total and cleaved caspase-3 and caspase-8 levels, which are typical biomarkers of cell death, were also significantly increased in the miR-506 overexpression group (Fig. 3a). These findings were also supported by the qPCR data (Fig. 3b). Furthermore, MRC-5 cells were treated with TGF-β1 protein to establish an in vitro lung fibrosis model. Annexin V-FITC and PI FC were then performed for assessing the extent of apoptosis. The results indicated that miR-506 expression enhanced the proportion of apoptotic MRC-5 cells, compared with those observed in the NC group (Fig. 3c).

## miR-506 inhibited inflammation of lung tissue in vivo during pulmonary fibrosis

As inflammation is one of the primary characteristics of pulmonary fibrosis (Cullinan and Reid 2013; Trentin et al. 2015), we evaluated the effects of miR-506 overexpression on the production of pro-inflammatory cytokines. Both WB and qPCR analyses showed that LPS treatment contributed to generation of pro-inflammatory cytokines (IL-6, IL-1β and TNF-α), whereas miR-506 overexpression restored them to a normal level (Fig. 4a, b).

## miR-506 targeted the 3′-UTR of p65

Further study showed that p65 levels were increased in the TGF-β-treated MRC-5 cell line at both the protein and mRNA levels, compared with that in non-treated cells (Fig. 5a, b). Furthermore, bioinformatics analyses showed that miR-506 may target the 3′-UTR of p65 (Fig. 5c). The direct interaction between miR-506 and the 3′-UTR of p65 was investigated using DLRA (Fig. 5d). The data showed that luciferase activity was suppressed by 70% compared with the control groups after the transfection of miR-506 mimic, which was fused with a 3′-UTR of p65. We then determined the effects of miR-506 expression on the p65 levels in TGF-β-treated MRC-5 cells using WB and qPCR. The protein and mRNA expression levels of p65 were remarkably decreased after the transfection of miR-506 mimic (Fig. 5e, f). The data demonstrated that p65 expression decreased after ectopic miR-506 overexpression and that miR-506 targeted the 3′-UTR of the p65 gene.

## P65 silencing ameliorated LPS-induced lung fibrosis

Next, we tested the effects of p65 silencing on fibrosis. WB and qPCR data confirmed the transfection of lentivirus-shRNA-p65, which led to the obvious reduction of p65 in LPS-treated mice at the protein and mRNA levels, respectively (Fig. 6a, b). Consistent with the lentivirus-miR-506 transfection results, p65 silencing significantly suppressed LPS-induced lung fibrosis in mice (Fig. 6c, d, e). The above findings demonstrated how miR-506 overexpression could suppress LPS-induced pulmonary fibrosis by modulating levels of p65. More importantly, we found that p65 knockdown in LPS-treated mice augmented the expression of E-cadherin, which was attenuated after LPS induction, at both the

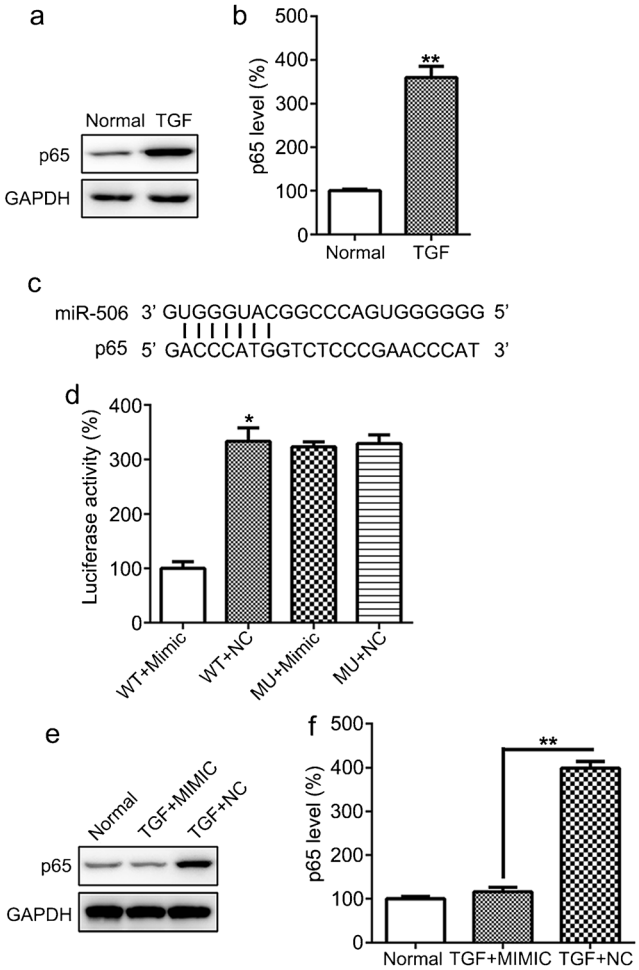


**Fig. 5** miR-506 targeted p65. WB (**a**) and qPCR analyses (**b**) were carried out to examine the upregulation of p65 in TGF-β1-treated MRC-5 cells. Explanatory chart (**c**) of the miR-506 binding motif at the 3′-UTR of p65. Luciferase activity (**d**) exhibited by the luciferase reporter constructs, which contained either the wild-type (WT) or mutated (MU) p65 3′-UTR after transfection with miR-506 mimic. The luciferase activities were normalized to those of β-galactosidase. WB analysis (**e**, **f**) was performed to evaluate p65 expression after transfection of TGF-β1-treated MRC-5 with miR-506-mimic or NC-mimic. Data are presented as the mean ± SD. $^{**}P < 0.01$, in comparison with the indicated group

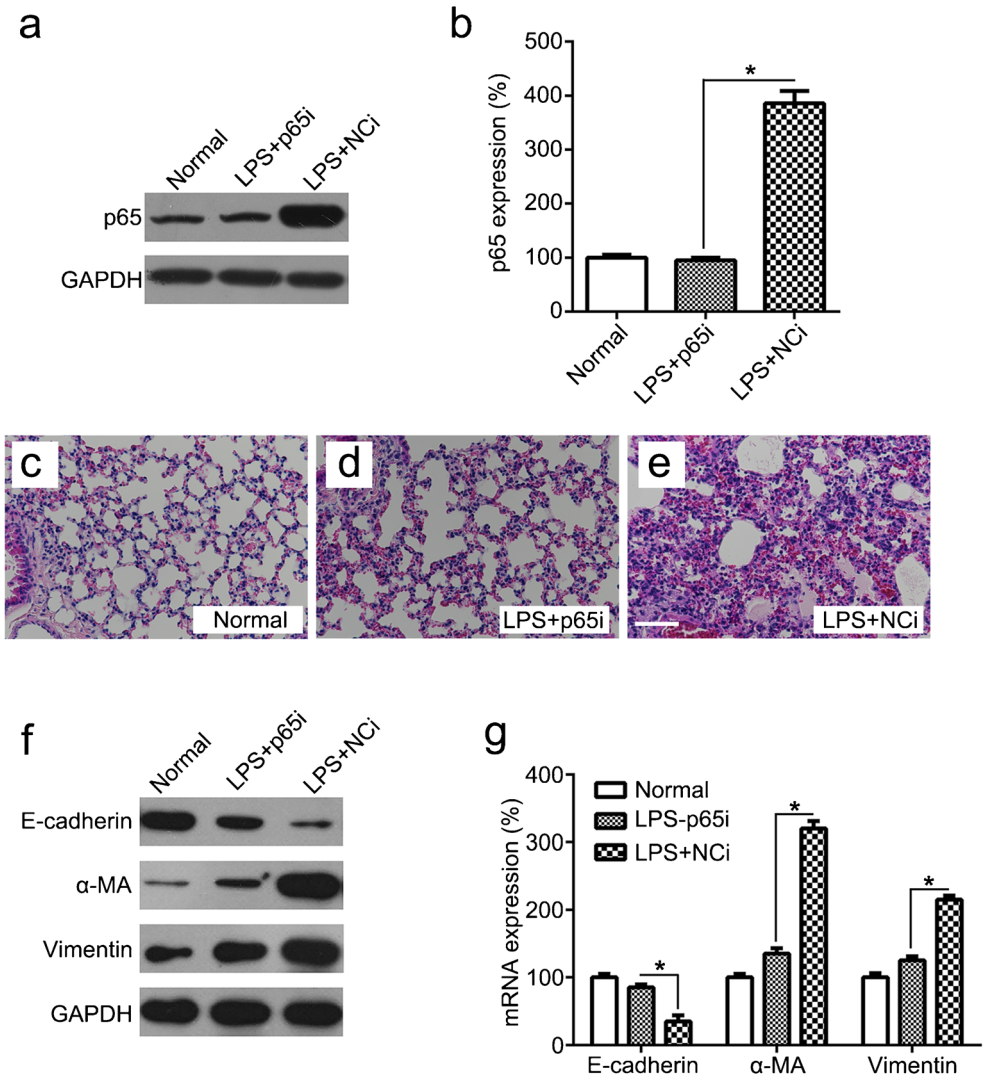


**Fig. 6** p65 silencing reduced the pathology of lung fibrosis in mice. Lentivirus-shRNA-p65 and lentivirus-shRNA-NC were injected intratracheally into the pulmonary tissue of C57BL/6 mice pretreated with LPS. WB (**a**) and qPCR (**b**) were performed to confirm p65 silencing. H&E staining (**c**, **d**, **e**) of lung tissue in mice with early lung fibrosis injected with lentivirus-shRNA-p65 and lentivirus-shRNA-NC. WB (**f**) and qPCR (**g**) analyses were carried out to examine the protein and mRNA levels of proteins associated with EMT (E-cadherin, α-MA and vimentin). Data are presented as the mean ± SD. $*P < 0.05$, in comparison with the indicated group. Scale bar, 20 μM

translational and transcriptional levels. We also found that p65 silencing significantly reduced α-MA and vimentin levels, compared with levels in the NC group (Fig. 6f, g).

We then investigated whether p65 silencing regulates apoptosis and inflammation, which have been observed to be mediated by miR-506 overexpression. WB and qPCR were utilized to validate the changes in apoptosis-associated protein expression following p65 silencing. The results showed that Bcl-2 levels were subsequently diminished after p65 silencing, compared with both the normal and NC group, while levels of Bax, caspase-3 and caspase-8 were significantly increased (Fig. 7a, b). We performed TUNEL assay to detect the apoptosis of lung sections. In the pulmonary fibrosis induced by LPS, an increase in alveolar epithelial cell apoptosis was observed. However, the lentiviral miR-506- and shRNA-p65-inoculated mice had significantly decreased TUNEL-positive cells compared with LPS-treated mice (Fig. 7c, d, e, f). Further, our data showed that p65 knockdown led to the production of pro-inflammatory cytokines promoted by LPS treatment. This was observed at a normal level in comparison to the NC group (Fig. 7g, h). ELISA was performed to detect the inflammatory mediators IL-6 production in lungs. Data showed that LPS treatment enhanced the production of IL-6, while inoculation with lentiviral miR-506 and p65 shRNA vector significantly reduced IL-6 generation (Fig. 7i). The results indicated that elevated miR-506 expression could promote apoptosis and suppress inflammation by regulating p65.

## Discussion

Our study revealed that miR-506 was downregulated in the lung tissue of a mouse model of LPS-induced pulmonary fibrosis. In mice, miR-506 overexpression suppressed lung fibrosis caused by LPS stimulation. Therefore, our investigation showed that miR-506 regulates a number of fibrogenic channels, through which lung fibrosis is mediated. All

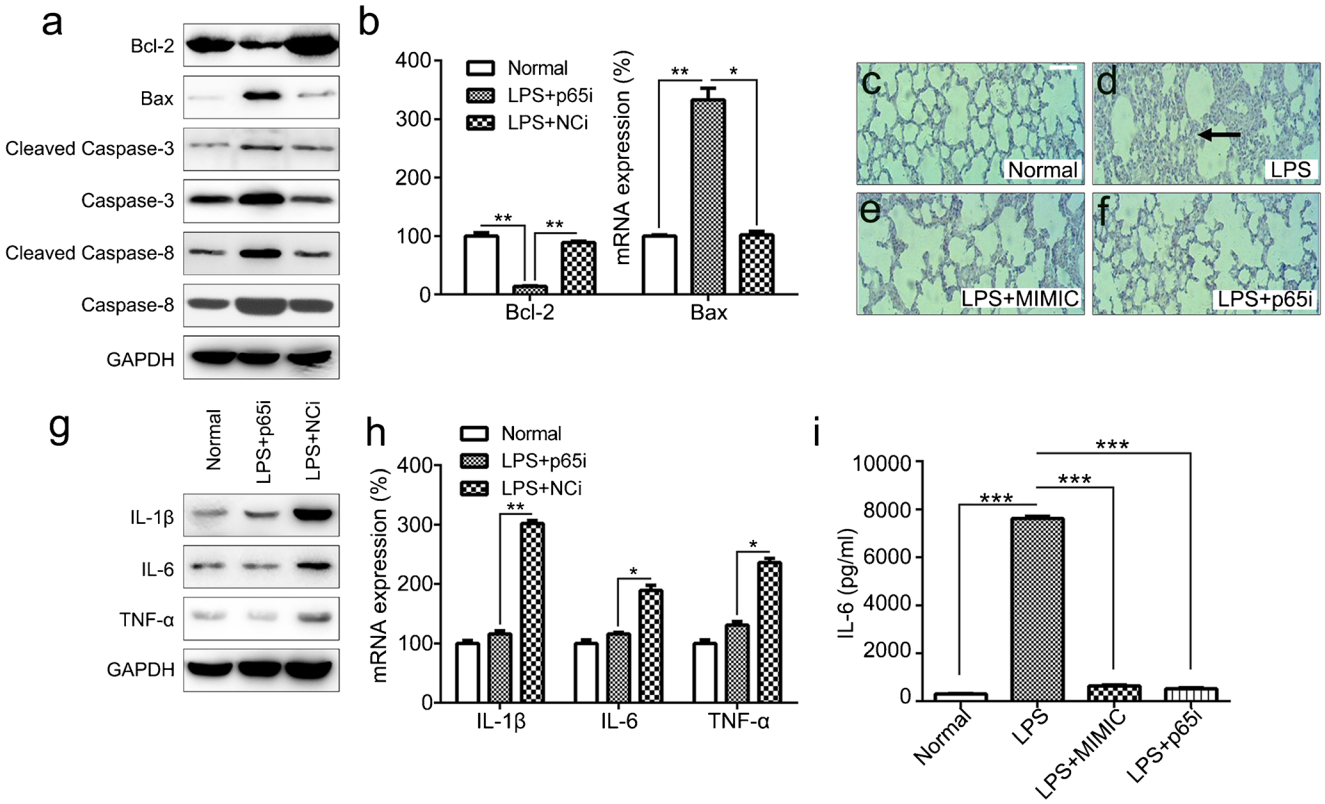


**Fig. 7** p65 silencing enhanced apoptosis and decreased inflammation in lung tissue of mice with lung fibrosis. Lentivirus-shRNA-p65 and lentivirus-shRNA-NC were injected intratracheally into the lungs of C57BL/6 mice pretreated with LPS. WB (**a**) was performed to evaluate the expression levels of Bax, Bcl-2, caspase-3, caspase-8 and their cleaved forms in the lung tissue. qPCR assay (**b**) was conducted to determine the mRNA levels of Bcl-2 and Bax. LPS-induced lung epithelial apoptosis detecting by TUNEL assay (**c**, **d**, **e**, **f**). Cellular apoptosis of lung epithelial cells was analyzed by TUNEL staining at 21 days post LPS treatment. Apoptotic cell nuclei are stained brown and marked by arrows. The LPS treatment mice exhibited significantly increased TUNEL-positive cells. Magnification, × 200. WB (**g**) and qPCR (**h**) assays were performed to evaluate the expressions of IL-6, IL-1β and TNF-α at the protein and mRNA levels, respectively. Reduction (**i**) of lung IL-6 levels detecting by ELISA. Lung IL-6 levels from healthy control mice and from rats with different treatments, as measured by ELISA. Data are presented as the mean ± SD. $*P < 0.05$, $**P < 0.01$, in comparison with the indicated group. Scale bar, 20 μM

experimental data demonstrated that miR-506 induced the apoptotic pathway and attenuates an inflammatory response by directly targeting p65, a subunit of NF-κB. Furthermore, miR-506 overexpression attenuated the expression of epithelial proteins in fibroblasts. Taken together, this study demonstrated that miR-506 serves as a major regulator of pro-fibrotic factors in the pulmonary epithelium. These factors regulate epithelial–mesenchymal interaction and influence the progression of pulmonary fibrosis.

After inducing fibrosis in mouse pulmonary tissue with LPS, alveolar construction and epithelial cells were impaired (Cao et al. 2018b). Furthermore, several pro-inflammatory cytokines were produced via impaired macrophages and epithelial cells (Kim et al. 2006). Our present study discovered that TGF-β1 levels in ARDS pulmonary tissue were significantly higher than that in the control group post-LPS treatment. Additionally, these levels eventually improved during the progression of early lung fibrosis. Therefore, TGF-β1 was associated with lung fibrosis and could promote the development of early lung fibrosis with LPS-triggered ARDS. The most important role of TGF-β1 during lung fibrosis is to recruit fibroblasts and stimulate their proliferation and EMT, which generates high levels of collagen and fibronectin (Luo et al. 2015). A previous study showed that TGF-β1 stimulates EMT in bladder carcinoma cells and enhances the expression levels of EMT-related genes (Zhuang et al. 2015). Our study also revealed abnormal levels of TGF-β1 after miR-506 overexpression. Therefore, there is a high probability of miR-506 indirectly regulating EMT progression by inhibiting the release of TGF-β1.

A number of studies have demonstrated that the apoptotic process may have a potential function in the pathogenic progression of lung lesions. The upregulation and downregulation of apoptosis are hypothesized to be crucial in the generation of lung fibrotic disorder (Uhal 2008), while inflammatory and fibrotic processes are two major traits of lung fibrosis (Cullinan and Reid 2013; Trentin et al. 2015). Our data showed that during lung fibrosis progression, apoptosis was suppressed and inflammation was induced. Moreover, our results suggested that excessive miR-506 expression weakened

pulmonary fibrosis in the mouse and suppressed TGF-β1-triggered fibrogenesis among MRC-5 cells by mediating apoptosis and inflammation. The aforementioned results demonstrated that miR-506 exhibits anti-fibrotic activity in pulmonary tissues and could serve as a new autophagy target in lung fibrosis therapy. Moreover, our current study validated that p65 is an miR-506 target, which is in agreement with earlier reports (Yin et al. 2015). P65 is an essential subunit of NF-κB, the signaling of which mediates multiple genes associated with cellular differentiation, multiplication, apoptosis and inherent immunoreaction. NF-κB initiates the transcription of anti-apoptotic genes (Gerondakis et al. 2006). Increasing evidence has suggested a critical role of NF-κB in apoptosis prevention during the progression of some cancers (Arlt et al. 2013; Gasparini et al. 2014; Nguyen et al. 2014). Activation of the NF-κB/Rel transcription group through nuclear transfer of cytoplasmic structures has a crucial function in inflammatory activities via its capability to trigger transcription of pro-inflammatory genes (Albert and Baldwin 1996; Gyrd-Hansen and Meier 2010), such as IL-6, IL-1β and TNF-α. The channel is activated by proper cell induction, often by signals of pathogens or stress. Further investigation revealed that p65 knockdown in mice with lung fibrosis caused a considerable decrease in lung fibrosis generation. These results demonstrated that p65 both triggered apoptosis and suppressed pro-inflammatory properties.

In conclusion, our findings indicated for the first time that lung fibrosis lesions and pathogenesis can be regulated by miR-506. The results also revealed that enhanced miR-506 expression in mice leads to the attenuation of LPS-mediated pulmonary fibrosis. Therefore, our results indicated that miR-506 is a key regulator in the pathogenic progression of pulmonary fibrosis. It is thus a promising target for developing novel therapeutic strategies against fibrotic disorders, including ARDS.

**Funding** This study was funded by the Youth Foundation of the National Natural Science Foundation of China (grant number 81600047).

## Compliance with ethical standards

**Conflict of interest** The authors declare that they have no conflict of interest.

## References

Albert S, Baldwin J (1996) The NF-κB and IκB proteins: new discoveries and insights. Annu Rev Immunol 14:649–681

Ambros V (2004) The functions of animal microRNAs. Nature 431:350–355

Arlt A, Muerkoster SS, Schafer H (2013) Targeting apoptosis pathways in pancreatic cancer. Cancer Lett 332:346–358

Arora H, Qureshi R, Park WY (2013) miR-506 regulates epithelial mesenchymal transition in breast cancer cell lines. PLoS One 8:e64273

Burnham EL, Janssen WJ, Riches DW, Moss M, Downey GP (2014) The fibroproliferative response in acute respiratory distress syndrome: mechanisms and clinical significance. Eur Respir J 43:276–285

Cao Y, Liu Y, Ping F, Yi L, Zeng Z, Li Y (2018a) miR-200b/c attenuates lipopolysaccharide-induced early pulmonary fibrosis by targeting ZEB1/2 via p38 MAPK and TGF-beta/smad3 signaling pathways. Lab Investig 98:339–359

Cao Y, Liu Y, Ping F, Yi L, Zeng Z, Li Y (2018b) miR-200b/c attenuates lipopolysaccharide-induced early pulmonary fibrosis by targeting ZEB1/2 via p38 MAPK and TGF-β/smad3 signaling pathways. Lab Investig 98:339

Carrington JC, Ambros V (2003) Role of microRNAs in plant and animal development. Science 301:336–338

Chapman HA (2011) Epithelial-mesenchymal interactions in pulmonary fibrosis. Annu Rev Physiol 73:413–435

Cullinan P, Reid P (2013) Pneumoconiosis. Prim Care Respir J 22:249–252

Cunningham AJ (1991) Acute respiratory distress syndrome–two decades later. Yale J Biol Med 64:387–402

Degryse AL, Tanjore H, Xu XC, Polosukhin VV, Jones BR, Boomershine CS, Ortiz C, Sherrill TP, McMahon FB, Gleaves LA, Blackwell TS, Lawson WE (2011) TGFβ signaling in lung epithelium regulates bleomycin-induced alveolar injury and fibroblast recruitment. Am J Physiol Lung Cell Mol Physiol 300:L887–L897

Ding XM (2014) MicroRNAs: regulators of cancer metastasis and epithelial-mesenchymal transition (EMT). Chin J Cancer 33:140–147

Gasparini C, Celeghini C, Monasta L, Zauli G (2014) NF-kappaB pathways in hematological malignancies. Cell Mol Life Sci 71:2083–2102

Gerondakis S, Grumont R, Gugasyan R, Wong L, Isomura I, Ho W, Banerjee A (2006) Unravelling the complexities of the NF-kappaB signalling pathway using mouse knockout and transgenic models. Oncogene 25:6781–6799

Gyrd-Hansen M, Meier P (2010) IAPs: from caspase inhibitors to modulators of NF-κB, inflammation and cancer. Nat Rev Cancer 10:561

Kang HR, Lee CG, Homer RJ, Elias JA (2007) Semaphorin 7A plays a critical role in TGF-beta1-induced pulmonary fibrosis. J Exp Med 204:1083–1093

Kim KK, Kugler MC, Wolters PJ, Robillard L, Galvez MG, Brumwell AN, Sheppard D, Chapman HA (2006) Alveolar epithelial cell mesenchymal transition develops in vivo during pulmonary fibrosis and is regulated by the extracellular matrix. Proc Natl Acad Sci 103:13180–13185

Lawson WE, Cheng DS, Degryse AL, Tanjore H, Polosukhin VV, Xu XC, Newcomb DC, Jones BR, Roldan J, Lane KB, Morrisey EE, Beers MF, Yull FE, Blackwell TS (2011) Endoplasmic reticulum stress enhances fibrotic remodeling in the lungs. Proc Natl Acad Sci U S A 108:10562–10567

Leask A, Abraham DJ (2004) TGF-beta signaling and the fibrotic response. FASEB J 18:816–827

Lee CG, Cho SJ, Kang MJ, Chapoval SP, Lee PJ, Noble PW, Yehualaeshet T, Lu B, Flavell RA, Milbrandt J, Homer RJ, Elias JA (2004) Early growth response gene 1–mediated apoptosis is essential for transforming growth factor β(1)–induced pulmonary fibrosis. J Exp Med 200:377–389

Li H, Du S, Yang L, Chen Y, Huang W, Zhang R, Cui Y, Yang J, Chen D, Li Y, Zhang S, Zhou J, Wei Z, Yao Z (2009) Rapid pulmonary fibrosis induced by acute lung injury via a lipopolysaccharide three-hit regimen. Innate Immun 15:143–154

Li M, Krishnaveni MS, Li C, Zhou B, Xing Y, Banfalvi A, Li A, Lombardi V, Akbari O, Borok Z, Minoo P (2011) Epithelium-specific deletion of TGF-beta receptor type II protects mice from bleomycin-induced pulmonary fibrosis. J Clin Invest 121:277–287

Li Z, Liu Z, Dong S, Zhang J, Tan J, Wang Y, Ge C, Li R, Xue Y, Li M, Wang W, Xiang X, Yang J, Ding H, Geng T, Yao K, Song X (2015) miR-506 inhibits epithelial-to-mesenchymal transition and angiogenesis in gastric cancer. Am J Pathol 185:2412–2420

Li J, Ju J, Ni B, Wang H (2016) The emerging role of miR-506 in cancer. Oncotarget 7:62778–62788

Luo Y, Xu W, Chen H, Warburton D, Dong R, Qian B, Selman M, Gauldie J, Kolb M, Shi W (2015) A novel profibrotic mechanism mediated by TGFβ-stimulated collagen prolyl hydroxylase expression in fibrotic lung mesenchymal cells. J Pathol 236:384–394

Marshall RP, Bellingan G, Webb S, Puddicombe A, Goldsack N, McAnulty RJ, Laurent GJ (2000) Fibroproliferation occurs early in the acute respiratory distress syndrome and impacts on outcome. Am J Respir Crit Care Med 162:1783–1788

Munger JS, Huang X, Kawakatsu H, Griffiths MJ, Dalton SL, Wu J, Pittet JF, Kaminski N, Garat C, Matthay MA, Rifkin DB, Sheppard D (1999) The integrin alpha v beta 6 binds and activates latent TGF beta 1: a mechanism for regulating pulmonary inflammation and fibrosis. Cell 96:319–328

Nguyen DP, Li J, Yadav SS, Tewari AK (2014) Recent insights into NF-kappaB signalling pathways and the link between inflammation and prostate cancer. BJU Int 114:168–176

Ragaller M, Richter T (2010) Acute lung injury and acute respiratory distress syndrome. J Emerg Trauma Shock 3:43–51

Richeldi L, du Bois RM, Raghu G, Azuma A, Brown KK, Costabel U, Cottin V, Flaherty KR, Hansell DM, Inoue Y, Kim DS, Kolb M, Nicholson AG, Noble PW, Selman M, Taniguchi H, Brun M, Le Maulf F, Girard M, Stowasser S, Schlenker-Herceg R, Disse B, Collard HR, Investigators IT (2014) Efficacy and safety of nintedanib in idiopathic pulmonary fibrosis. N Engl J Med 370: 2071–2082

Rockey DC, Bell PD, Hill JA (2015) Fibrosis–a common pathway to organ injury and failure. N Engl J Med 373:96

Sime PJ, Xing Z, Graham FL, Csaky KG, Gauldie J (1997) Adenovector-mediated gene transfer of active transforming growth factor-beta1 induces prolonged severe fibrosis in rat lung. J Clin Invest 100:768–776

Sun Y, Mezzanzanica D, Zhang W (2014) MiR-506: a multitasker in suppression of the epithelial-to-mesenchymal transition. RNA Dis 1:e447

Trentin PG, Ferreira TP, Arantes AC, Ciambarella BT, Cordeiro RS, Flower RJ, Perretti M, Martins MA, Silva PM (2015) Annexin A1 mimetic peptide controls the inflammatory and fibrotic effects of silica particles in mice. Br J Pharmacol 172:3058–3071

Uhal BD (2008) The role of apoptosis in pulmonary fibrosis. Eur Respir Rev 17:138–144

Woessner J Jr (1961) The determination of hydroxyproline in tissue and protein samples containing small proportions of this imino acid. Arch Biochem Biophys 93:440–447

Yang X-P, Li Y, Wang Y, Wang Y, Wang P (2010) β-Tryptase up-regulates vascular endothelial growth factor expression via proteinase-activated receptor-2 and mitogen-activated protein kinase pathways in bone marrow stromal cells in acute myeloid leukemia. Leuk Lymphoma 51:1550–1558

Yao J, Qin L, Miao S, Wang X, Wu X (2016) Overexpression of miR-506 suppresses proliferation and promotes apoptosis of osteosarcoma cells by targeting astrocyte elevated gene-1. Oncol Lett 12:1840–1848

Yin M, Ren X, Zhang X, Luo Y, Wang G, Huang K, Feng S, Bao X, He X, Liang P (2015) Selective killing of lung cancer cells by miRNA-506 molecule through inhibiting NF-κB p65 to evoke reactive oxygen species generation and p53 activation. Oncogene 34:691

Zhang HY, Gharaee-Kermani M, Zhang K, Karmiol S, Phan SH (1996) Lung fibroblast alpha-smooth muscle actin expression and contractile phenotype in bleomycin-induced pulmonary fibrosis. Am J Pathol 148:527–537

Zhuang J, Lu Q, Shen B, Huang X, Shen L, Zheng X, Huang R, Yan J, Guo H (2015) TGFβ1 secreted by cancer-associated fibroblasts induces epithelial-mesenchymal transition of bladder cancer cells through lncRNA-ZEB2NAT. Sci Rep 5:11924